

## A THREE-DIMENSIONAL CFD MODEL FOR COAL BLENDS COMBUSTION: MODEL FORMULATION AND VALIDATION

Y.S. SHEN<sup>1</sup>, B.Y. GUO<sup>1</sup>, P. ZULLI<sup>2</sup>, D. MALDONADO<sup>2</sup> and A.B. YU<sup>1</sup>

<sup>1</sup> School of Materials Science and Engineering, University of New South Wales, Sydney, NSW 2052, Australia

<sup>2</sup> Bluescope Steel Research, P.O. Box 202, Port Kembla, NSW 2505, Australia

### ABSTRACT

Coal blends combustion is widely practised in blast furnace ironmaking and in coal-fired power stations. It is desirable to be able to characterize the burning performance of coal blends prior to full scale trials. A three-dimensional numerical model is developed to simulate the flow and combustion of a binary coal blend, and validated using measurements from a pilot-scale combustion test rig for three cases. Rather than treating the blend as a single coal with weighted-average properties of its components, in this model, the two component coals in the blend, with individual properties, are tracked separately and undergo individual chemical reactions using individual kinetics. As a result, this model is capable of providing individual information of component coals. In addition, this model includes coaxial lance and three gas streams. Flow pattern features are simulated and combustion behaviours in the combustor are predicted in terms of burnout, particle temperature and volatile content.

Keywords: coal blends, coal combustion, CFD modelling, blast furnace.

### NOMENCLATURE

$e$	void fraction
$Nu$	Nusselt number
$Pr$	Prandtl number
$R$	particle radius
$Re$	Reynolds number
$T_c$	activation temperature
$v_i$	velocity for fluid and particle
$\Gamma$	a normally distributed random number
$\rho$	density
$\sigma$	Stefan-Boltzmann constant
$k$	turbulent kinetic energy
$\varepsilon$	turbulence dissipation rate

### INTRODUCTION

Combustion of pulverized coal blends is widely practised in blast furnace ironmaking (Stainlay and Bennett, 2001; Bennett, 2001) and coal-fired power plants (Carpenter, 1995; Wall *et al.*, 2001). In blast furnace ironmaking, pulverized coal injection (PCI) through tuyeres into furnace raceway is used to lower operating costs and to maintain furnace operation stability. Coal blends enables better control of coal quality and allows selection of a blend to optimise combustion. While as the levels of coal rate increases, the burnout of coal within the tuyere and raceway becomes increasingly important, as unburnt char,

with ash, impacts on the permeability of the raceway boundary and ultimately on the furnace stability (Saxen *et al.*, 2001; Shen *et al.*, 2002). In coal-fired boiler in power stations, coal blending is widely used to improve coal flexibility, improve combustion behaviours, mitigate operation problems (e.g. ash deposition), and reduce pollutants emissions. Similar to the blast furnace, coal combustion is rarely completed in boilers and the uncompleted burning affects the operation of the power plant (Carpenter, 1995). Therefore, it is desirable to be able to characterize the burnout behaviours of the coal blends prior to full scale trials in both industries.

CFD modelling provides an accurate and cost effective tool for optimizing operation and lance/burner design. In particular, it can provide insight into the combustion characteristics of unfamiliar coals and blends. For this reason, CFD is widely employed to evaluate the combustion performance of single coal in blast furnace raceway, summarised by Ishii (2000), and in power plant boiler (for instance, Jones *et al.*, 1999 etc.). While the combustion performance of a coal blends is more complex than that of a single coal because it is not only dependent on the combustion performance of the component coals but also on the physical/chemical interactions between coal particles. Unfortunately, very few CFD models (Arenillas *et al.*, 2002; Beeley *et al.*, 2000; Sheng *et al.*, 2001) are found for coal blends in open literature. But the previous modelling works consist of two-dimensional models or consider the coal blends simply as one single coal using averaged properties of component coals. Three-dimensional modelling is needed to generate quantitatively realistic information. In addition, none of the previous models are applicable to the operational features of PCI in a blast furnace, where the different lance design affects the combustion of coals.

In the present model, to overcome these problems, a three dimensional model for coal blends combustion is developed to simulate the flow pattern and combustion performance of a binary coal blends. Compared with the previous models of coal blends combustion, in this work, in a blend, two different types of coals, with varying physical and chemical properties, are considered and tracked separately, and two component coals undergo individual reactions using individual reaction kinetics, and interact through local competition for oxygen supply. Therefore, this model is able to generate individual information for component coals. In addition, different from the previous models, this model involves the geometric details of the lance design associated with PCI operation in blast furnace, including an inclined coaxial

lance and three gas streams (conveying gas, cooling gas and hot blast air). The model is then validated against the experimental measurements obtained from a pilot-scale combustion rig in terms of coal burnout for three binary coal blend cases. Therefore, this model offers an effective tool to predict the combustion behaviour of coal blends, especially blends of unfamiliar coals or blends of three or more coals. Due to page limit, this paper presents the model formulation, model validation and general analysis on typical results. The behaviours of two component coals and parametric study will be reported in future work.

## MODEL DESCRIPTION

### Governing Equations for Gas Phase

The gaseous field is described by the transport equations of the continuum phase. Three-dimensional, steady-state Reynolds averaged Navier-Stokes equations closed by the k- $\epsilon$  turbulence model are solved for the turbulent gas flow, including mass, momentum, turbulence kinetic energy, turbulent dissipation rate, enthalpy, and a number of gaseous species mass fractions.

### Particle Transport

In this model, two coal particle groups are employed to track the individual component coals (Coal1 and Coal2) separately. Rather than being modelled as an extra Eulerian phase, two distinct injections of particles are treated as dispersed phases in a Lagrangian way, by which particle behaviours are tracked along the discrete particle trajectories without considering physical interaction between particles in gas phase.

The forces acting on the particle which affect the particle acceleration include drag force, pressure gradient force, virtual mass force, buoyancy force and turbulent dispersion *etc.* In this model, only the drag force and turbulent dispersion are modelled. The drag force is calculated by,

$$F_D = \frac{1}{8} \pi d^2 \rho_f C_D |v_f - v_p| (v_f - v_p) \quad (1)$$

The drag coefficient  $C_D$  is given by modified Schiller and Naumann (1933),

$$C_D = \max(24(1 + 0.15 \text{Re}^{0.687}) / \text{Re}, 0.44) \quad (2)$$

The turbulent dispersion of particles is modelled by assuming that a particle is within a single turbulent eddy. Each eddy has a characteristic fluctuating velocity,  $v_f'$ , lifetime,  $\tau_e$ , and length,  $l_e$ . They are calculated by (Gosman and Ioannides, 1981),

$$v_f' = \Gamma(2k/3)^{0.5} \quad (3)$$

$$l_e = C_\mu^{0.75} k^{1.5} / \epsilon \quad (4)$$

$$\tau_e = l_e / (2k/3)^{0.5} \quad (5)$$

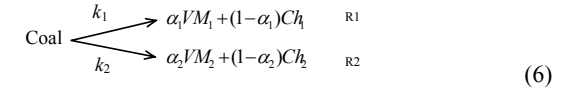
The coal particles are considered as non-interacting spheres with uniform temperature and composition. Full coupling of mass, momentum and energy of particles with the gaseous phase is applied, such that the fluid is allowed to influence trajectories and the particles also affect the fluid behaviour. In addition, a swelling model is used for the diameter change of raw coal during coal pyrolysis.

### Devolatilisation

In general, coal combustion is considered as a three-stage process: the devolatilization of a raw coal particle, followed by the gaseous combustion of the volatiles and

the oxidation of the residual char in the gas phase. In the present study dealing with coal blends, the blends combustion involves two chemically different fuels. Two component coals with different properties will undergo individual combustion reactions, including devolatilization, gaseous combustion and char oxidation.

Devolatilization is modelled using the generic Arrhenius reactions capability. In this study, the model proposed by Ubhayakar (1976) is used, in which a pair of reactions with different rate parameters and volatile yields compete to pyrolyse the raw coal.



The first reaction dominates at lower temperatures with a lower yield  $\alpha_1$  than the yield  $\alpha_2$  of the second reaction (dominating at higher temperatures,  $> \sim 1200$  K). The yields are defined on a dry ash-free (daf) basis. The rate constants  $k_1$  and  $k_2$  are in Arrhenius format,

$$k = A \exp(-E/T_p) \quad (7)$$

where Arrhenius rate constant,  $A$ , and activation energy,  $E$ , for the first devolatilisation reaction are  $3.7 \times 10^5 \text{ s}^{-1}$  and  $18000 \text{ K}$ , respectively, and for the second one,  $1.46 \times 10^{13} \text{ s}^{-1}$  and  $30189 \text{ K}$ , respectively (Aoki et al., 1993).

### Char Oxidation

The second coal pyrolysis product is char. Char combustion is a much slower process than devolatilization, and it therefore determines the burnout time of the coal in the raceway. Char oxidation is modelled using the model proposed by Gibb (1985), where besides the external diffusion the diffusion of oxygen within the pores of a char particle is also considered. By solving the oxygen diffusion equation analytically, the following equation is obtained for the rate of decrease in the char mass  $m_c$ :

$$\frac{dm_c}{dt} = -\frac{3\phi}{1-e} \frac{M_C}{M_{O_2}} \frac{\rho_\infty}{\rho_C} (k_1^{-1} + (k_2 + k_3)^{-1})^{-1} m_c \quad (8)$$

where  $\phi$  is assumed to depend on the particle temperature.  $M_C$  is the molecular weight of carbon and  $M_{O_2}$  is the molecular weight of oxygen molecule.  $k_1$  is the rate of external diffusion,  $k_2$  is the surface reaction rate, and  $k_3$  is the rate of the internal diffusion and surface reaction.

$$k_1 = \frac{D}{R_p^2}, \quad k_2 = (1-e) \frac{k_c}{R_p}, \quad k_c = A_c T_p \exp\left(-\frac{T_c}{T_p}\right),$$

$$k_3 = k_c T_p (\beta \coth \beta - 1) / \beta^2 a, \quad \beta = R \left(\frac{k_c}{D_p e a}\right)^{0.5},$$

where  $D_p$  is computed from external diffusivity,  $D$ .  $k_c$  is the carbon oxidation rate, defined by the modified Arrhenius equation. The constants are  $A_c = 14 \text{ m/s}$  and  $T_c = 21580 \text{ K}$  (Gibb, 1985).

### Gaseous Combustion

Besides the volatiles, other major gaseous species considered in this model are  $O_2$ ,  $CO_2$  and  $N_2$ , which could be generated from various homogenous and heterogenous reactions during coal combustion. The Gas phase combustion reactions are modelled by means of regular single phase reactions, using the eddy dissipation model (Magnussen et al., 1979). The contribution of radiation to enthalpy transport is modelled by the discrete transfer model. The gas compositions are obtained from the

solution of transport equations for the mass fraction of the elements. These equations contain sources and sinks due to the homogenous and heterogenous reactions.

### Heat Transfer

The radiative heat transfer, concerned with coal and char, is one of the most significant features of coal combustion compared with gaseous and liquid combustion. The net radiative power absorbed by a particle with diameter  $d_p$ , uniform temperature  $T_p$  and emissivity  $\epsilon_p$  is calculated by,

$$q_r = 0.25\epsilon_p\pi d_p^2(I - \sigma T_p^4) \quad (9)$$

where  $I$  is the radiative flux at the location of the particle as calculated in the radiation solver. The value of the particle emissivity  $\epsilon_p$  is expected to change as pyrolysis proceeds, i.e., it varies depending upon the mass fractions of coal and char. The present model assumes a linear variation in  $\epsilon_p$  from the raw coal value  $\epsilon_p$  (coal) to the value for char  $\epsilon_p$  (char). That is,

$$\epsilon_p = (1 - f_v)\epsilon_p(\text{coal}) + f_v\epsilon_p(\text{char}) \quad (10)$$

where  $f_v$  is the fractional yield of volatiles. Typical values for  $\epsilon_p$  are 1.0 for coal and 0.6 for char.

Another significant heat transfer mode is convection. It is assumed that the combustion of volatiles releases heat into the gas phase and the oxidation of char releases heat into the coal particles. Convective heat transfer due to temperature difference between the fluid and a particle is calculated using a semi-empirical correlation for the Nusselt number according to Ranz-Marshall (1952),

$$Nu = 2 + 0.6Re^{0.5} Pr^{0.33} \quad (11)$$

### METHOD OF SOLUTION

The simulation geometry for the coal combustion model is shown in Figure 1, based on a pilot-scale combustion test rig. The geometry and boundary conditions are regarded as plane-symmetric. A boundary fitted, multi-block structured finite volume mesh is generated, with the mesh points refined at the lance tip region for high variation. A smooth wall, a no-slip flow and adiabatic heat transfer are applied as boundary condition for gas phase and solid phase. The model is solved using ANSYS-CFX10.0.

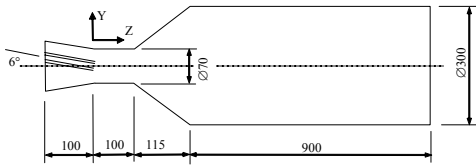


**Figure 1:** Main dimensions (mm) of the model.

In this study, the binary coal blends consists of two types of component coals, with different physical and chemical characteristics. The individual properties of the two coal groups, including proximate and ultimate analysis on air dried (ad.) basis, are summarized in Table 1. In this study, Rosin Rammler distribution is used to describe the particle size distribution of coals (Table 1). The mass fraction,  $R$ , above a given particle diameter,  $d$ , is calculated from,

$$R = \exp\left[-(d/d_e)^\gamma\right] \quad (12)$$

where  $d_e$  is a measure of the fineness, and  $\gamma$  is a measure of size dispersion (Yu and Standish, 1990).

	Coal1	Coal2
moisture, %	3.2	1.2
volatile matter, %	32.5	19.95
ash, % (ad)	9.8	9.7
fixed carbon, %	54.5	69.1
sulphur total, %	0.58	0.34
gross specific energy, cal/kg	7185	7629
C, %	83.5	89.1
H, %	5.3	4.7
N, %	1.95	1.7
S, %	0.6	0.37
O, %	8.6	4.1
$d_e$ , $\mu\text{m}$	63	41

**Table 1:** Proximate and ultimate analysis of the components coals (ad.)

In order to simulate the coal blends combustion in PCI operation of blast furnace, additional features for the lance arrangement and structure are considered: 1) the lance is introduced into the duct upstream of the tuyere at an inclination of 6 degree to the duct centreline with its tip on the centreline; 2) three gas streams (conveying gas, cooling gas and hot blast) are introduced into the domain. The flow rates for three streams are based on the experimental conditions summarized in Table 2.

	flow rate	temperature
blast (20.9% O <sub>2</sub> )	300 Nm <sup>3</sup> /h	1473 K
cooling gas (20.9% O <sub>2</sub> )	3.2 Nm <sup>3</sup> /h	600 K
conveying gas (100% N <sub>2</sub> )	2.0 Nm <sup>3</sup> /h	323 K
coal rate	23.2, kg/h	
blend ratio	Coal1 50%	320 K
	Coal2 50%	

**Table 2:** Basic boundary conditions for computation

## RESULTS AND DISCUSSION

### Model Validation

The model is validated in terms of the overall burnout of blends using the measurements from a pilot-scale test rig (Rogers *et al.*, 2006), for three coal blends cases under various conditions.

The coal blends combustion properties, including particle temperature (T), burnout (B) and volatile content (VM) are calculated along the central tube (The mass-weighted mean values are calculated by averaging the properties over all the particles passing a circular cross-section with a small diameter of 50mm). The burnout B, which is a measure of the extent of coal combustion, is calculated using an ash balance:

$$B = (1 - \frac{m_{a,0}}{m_a}) / (1 - m_{a,0}) \quad (13)$$

where  $m_{a,0}$  is the ash content of the original coal and  $m_a$  is the ash content of the burnt residual collected. Both values are on a dry basis (db) in order to compare with the test data, although the moisture is released together with the other volatiles in the model. As defined, the burnout represents the total weight loss of the organic fraction of the coal due to volatile release and char reaction.

Three blends combustion cases are carried out to validate the model in terms of overall burnout at the distance of

925mm from lance tip under various experimental conditions, resulting in their O/C ratio ranging from 2.19 to 3.78. Table 3 summarizes the experimental conditions of three cases. Table 4 compares the predicted B and the measured B for each case. It shows that, for each case the predicted overall burnout at 925mm agrees well with the measured one, for both low and high O/C ratio.

case	blast rate, Nm <sup>3</sup> /h	blast temp., C	O <sub>2</sub> , %	coal rate, kg/h
base	300	1200	21.0	23.2
2	301	1199	21.1	38.2
3	296	1200	25.9	47.6

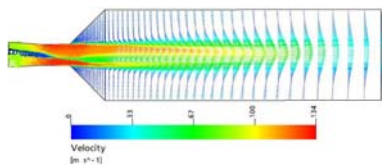
**Table 3:** Experimental conditions of three validating cases

case	O/C	central B at 925mm, %		error, %
		measured	predicted	
base	3.78	76.3	78.63	+2.96
2	2.28	71.5	72.42	+1.27
3	2.19	71.4	72.65	+1.72

**Table 4:** Model validation in terms of burnout for three cases under various experimental conditions

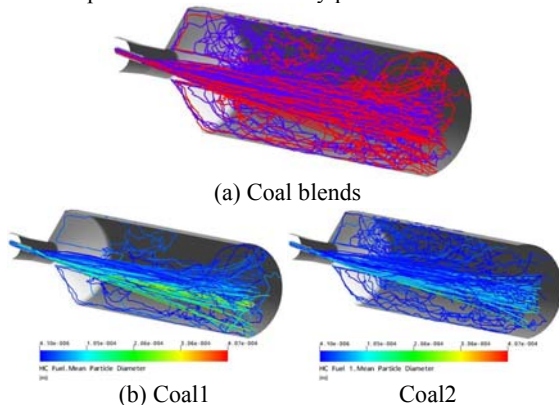
### Gas Flow and Particle Trajectories of Component Coals

Figure 2 shows the gas phase velocity vectors on the symmetry plane of the base blends case. It shows: 1) after exiting the tuyere, the gas stream forms a high-speed, inclined central jet, which then expands in the radial direction. 2) a large-scale recirculation occurs near the wall.



**Figure 2:** Gas velocity vectors along the symmetry plane.

Figure 3 shows the representative particle trajectories: (a) coal blends, where Coal2 is in blue and Coal1 is in red; (b) two component coals coloured by particle mean diameter.



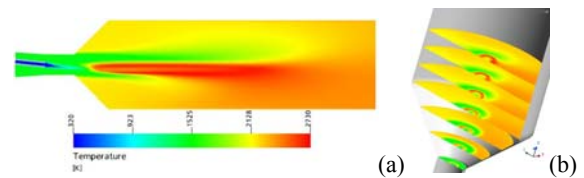
**Figure 3:** Typical particle trajectories of coal blends and two component coals.

They show: 1) in the chamber, the particle trajectories form an inclined plume due to the inclined lance arrangement, similar to the gas field; 2) particles below a certain size recirculate near the wall (Figure 3 (b)); 3) comparing the individual trajectories for the two

component coals, it can be seen that, the individual trajectories for two component coals give much difference in segregation: Coal2 has a greater level of dispersion (towards the wall) than Coal1, and is therefore more easily entrained into the recirculating flow region. This is because, Coal2 has a finer particle size distribution than Coal1 (Table 1). After exiting the lance, the large particles with high momentum maintain their initial direction, while the finer particles tend to be entrained in the gas flow and then travel in the main stream direction. The finer particles also disperse more widely, due to the fact that they have lower inertia and are more easily affected by turbulence.

### Combustion behaviours of Coal Blends

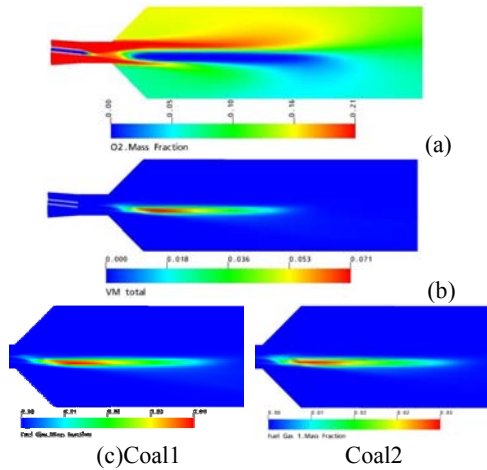
Figure 4 shows the gas temperature distribution of the base coal blends case on the symmetry plane (a) and the slices showing the flame front (b). Figure 4 (a) shows an asymmetric temperature distribution due to the inclined lance arrangement and the resultant combusting coal plume, higher temperature in the lower part; Figure 4 (b) shows an annular zone (flame front) of high temperature, this is because, at the surface of the coal plume, rapid burning of volatiles releases much heat due to sufficient oxygen supply locally.



**Figure 4:** Gas temperature contour on symmetric plane (a) and slices showing flame-front (b).

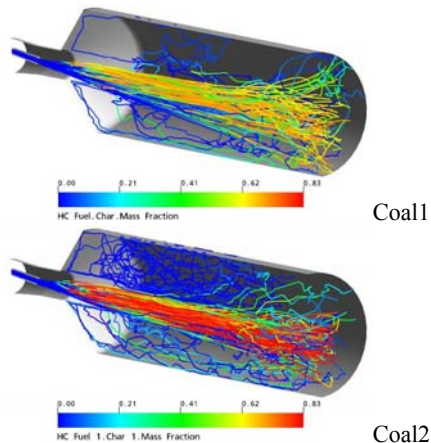
Figure 5 shows the oxygen (a) and volatile matter (b) mass fractions of the coal blends, and the individual information of two component coals (c), along the symmetry plane in the base coal blends case. Figure 5 (a) shows the oxygen concentration in the coal plume region is always low as the combustion of the volatile and char oxidation consume oxygen. Thus it can be indicated that the supply of oxygen primarily controls the combustion process.

Figure 5 (b) shows a build-up of volatile content in the core of the coal plume near tuyere exit. This is because, after exiting tuyere, the fuel-rich core is surrounded by a high temperature reaction zone (see Figure 4). This high temperature zone promotes a rapid generation of volatile gases. On the other hand, this zone is also oxygen-depleted zone (see Figure 5 (a)), thus the volatile gases are not immediately consumed by oxygen. Beyond this zone, volatile matter is consumed up by sufficient oxygen supply quickly. As a result, the overall volatile matter builds up in this zone. The individual contributions from two component coals, Coal1 and Coal2, on the total volatile matter of coal blends can be obtained by this model, shown in Figure 5 (c). They show that, in this coal blends combustion, Coal1 contributes ~4/7 of the total volatile matter and Coal2 contributes ~3/7. This is because Coal1 has higher volatile matter, as shown in proximate analysis (Table 1) and is able to generate more volatile matter than Coal2 under the same temperature environment.



**Figure 5:** Oxygen and volatile mass fractions of coal blend and two component coals along the symmetry plane.

Figure 6 gives the individual information of char mass fractions for Coal1 and Coal2 along their representative trajectories. The centre region and the wall region show different behaviours, resulting from local char generation and depletion: 1) along the centre plume, initially, the char mass fraction increases fast near tuyere exit due to fast devolatilization under high temperature, similar with volatile matter, but beyond this zone, i.e., downstream, different from volatile matter pattern, the char mass fractions keep increasing but slowly as the slow char oxidation becomes dominate. Coal2 shows higher char mass fraction than Coal1 due to its higher fix carbon in proximate analysis (Table 1); 2) at the region close to wall, i.e., the recirculation region of the fine particles, char mass fractions of Coal1 and Coal2 are quite low due to strong char oxidation and long resident time for fine particles.



**Figure 6:** Individual information of two component coals, in terms of char mass fraction

Figure 7 shows the evolution of coal blends with distance from the lance tip in terms of T, B and VM ((a), (b), (c) for all particles, and (d), (e), (f) for different size groups).

It is found in (a), (b) and (c) that, 1) T increases consistently along the central tube with distance from lance tip, rapidly up to 0.5m and but slowly beyond 0.5 m; 2) VM is approximately constant up to 0.05m, then decreases rapidly to a low level beyond 0.4m; 3) after

0.05m, B increases rapidly until 0.3-0.4m downstream from the lance, where there is a significant transition, followed by a levelling off at ~70-80% approximately. The explanation of this transition is as follows. Before the transition, the temperature of the coal particles increases fast due to downstream radiation. The raw coal particles start to release volatile (devolatilization) at ~0.05m and proceeds rapidly. As a result of rapid volatile combustion, particles are heated up rapidly to 2400K and the overall burnout increases quickly to 70%-80%. However, beyond the transition (greater than 0.4m), slow oxidation of the char particles controls the process and the rate of increase in burnout decreases. In these processes, two component coals interact chemically through local competition for oxygen supply. Therefore, from the general analysis on overall combustion properties of T, B and VM, it can be concluded, the devolatilization is primarily responsible for enhancing burnout level.

It is found in (d), (e) and (f) that, all properties including T, B and VM of particles are strongly dependent on particle size. 1) Regarding devolatilization, at 0.2 m, particles below 30  $\mu\text{m}$  have nearly completed devolatilisation, whereas those above 80  $\mu\text{m}$  have barely started. 2) Regarding particle temperature T, finer particles have higher T than larger particles. However this is not always the case. Beyond 0.2m, particle groups in the size range of 1-10  $\mu\text{m}$  and 10-20  $\mu\text{m}$  no longer undergo a high heating rate and level off around 2400K. Moreover, it is found that the size group in the 1-10  $\mu\text{m}$  range even reaches a lower temperature than the group in the 10-20  $\mu\text{m}$  particle range. This is not the case with the larger particle groups which take longer distances to undergo heating. This is because, compared with large particles, small particles have a higher surface area/mass ratio, leading to a faster temperature rise. Coal commences devolatilization at approximately the same temperature of ~1000 K for all particle sizes, thus for large particles, this process is delayed. For fine particles, especially beyond 0.2m, smaller particles (<20 $\mu\text{m}$ ) have higher B than coarse ones, even reaching a high level of ~90% (Figure 7 (e)), nearly burning off. Thus, compared with coarser particles, beyond 0.2m, fine particles of less than 20  $\mu\text{m}$  lose the chance to be heated to a temperature as high as the coarser particles.

3) Regarding burnout B, for each size group curve, it is found a transition occurs on each curve, from a rapid increase to a levelling off. Also, for each curve, it is found that devolatilization is the main contributor to coal burnout level, as discussed above. On the other hand, when comparing the burnout evolution for various size groups in Figure 7 (e), it is found, both the rate of increase of the burnout curve and the level of the curve are significantly dependent on particle sizes. Particles less than 20  $\mu\text{m}$  start to burn almost immediately within the tuyere (<~0.1m), followed by a higher rate of increase in burnout, reaching a higher burnout level than the larger particles. On the other hand, large particles over 80  $\mu\text{m}$ , only start to burn after leaving the tuyere (>~0.3m), followed by a slower rate of increase, reaching a lower burnout value than the fine particles. In other words, before the transitions, fine particles start to burn earlier and have earlier and faster increase than coarse ones. This sequence results from the sequence of devolatilization for the various size groups. However, beyond the transitions,

when char oxidation controls the burning process, it is found, fine particles have higher burnout level than coarse ones due to the fact that, fine particles experience higher temperature and as a result have higher reaction rate than coarse ones. Therefore, it can be indicated that, for the coal of a given VM content, concerning its various size groups, a size group of smaller particles has an earlier and faster increase and reaches a higher burnout level than large ones.

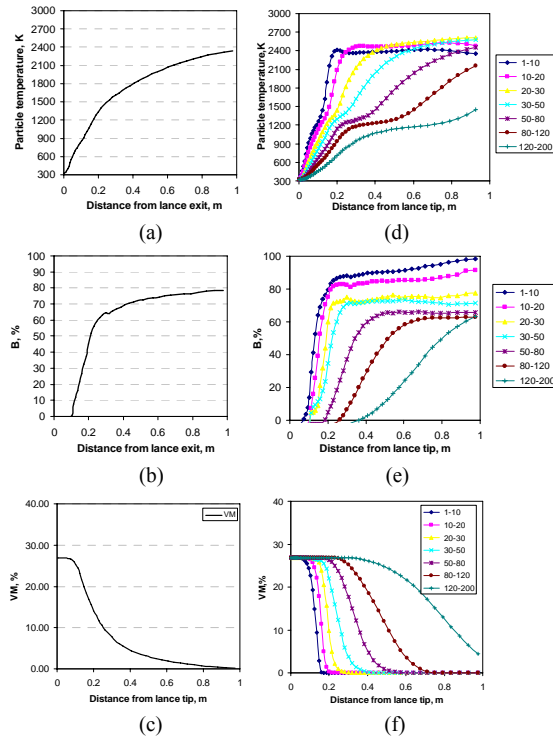


**Figure 7** Evolution of particle properties with distance from lance tip (overall: T (a), B (b) and VM (c), and for different particle size groups: T (d), B (e) and VM (f)).

The individual information and interactive behaviours of two component coals and parametric study will be reported in future work due to page limit.

## CONCLUSION

A three dimensional CFD model is developed for simulating the flow and combustion of coal blends in a blast furnace raceway cavity. The model includes two distinct groups of component coals in a blend to track the component coals individually. The two component coals undergo individual reactions separately using individual kinetics. In addition, this model includes geometric details of lance associated with PCI operation in blast furnace raceway cavity. The model is validated against the measurements of coal burnouts from a pilot-scale test rig.

The results show that, 1) the flow pattern and combustion behaviours are reproduced, such as flow asymmetry, recirculation flow, segregation of two component coals, particle dispersion, flame front temperature; 2) devolatilization process is largely responsible for enhancing the level of burnout; 3) both the increase rate of burnout and the burnout level are significantly dependent on particle size as a function of distance from the lance tip. For a coal of a given VM content, for the various size

groups, finer particles under faster devolatilisation give faster burnout increases and reach higher burnout levels;

## ACKNOWLEDGEMENT

The authors wish to thank the financial support from Endeavour International Postgraduate Research Scholarship (EIPRS) and Bluescope Steel, and the experimental data provided by Dr. Rogers Harold of BHP-Billiton.

## REFERENCES

- ANSYS CFX, CFX10.0 Online Document.
- ARENILLAS, A., BACKREEDY, R.I., JONES, J.M., PIS, J.J., POURKASHANIAN, M., RUBIERA, F., WILLIAMS, A., (2002), "Modelling of NO formation in the combustion of coal blends", *Fuel*, **81**, 627.
- BEELEY, T., CAHILL, P., RILEY, G., STEPHENSON, P., LEWITT, M., Whitehouse, M., (2000), "The effect of coal blending on combustion performance", *DTI Report No. COAL R177, DTI/Pub URN 00/509*, London.
- BENNETT P., (2001), "Combustion of coal blends", *the Pittsburgh coal conference*, Newcastle, Australia, December 2001.
- CARPENTER, A.M., (1995), "Coal blending for power stations", *IEA Coal Research*, London.
- GIBB, J., (1985), "Combustion of Residual Char Remaining after Devolatilization", *Lecture at Course of Pulverised Coal Combustion*, Imperial College, London.
- GOSMAN, A.D. and IOANNIDES, E., (1983), *J. Energy*, **7**, 482.
- ISHII, K., (2000), "Advanced Pulverised Coal Injection Technology and Blast Furnace Operation", Elsevier Science Ltd.
- JONES, J.M., PATTERSON, P.M., POURKASHANIAN, M., WILLIAMS, A., ARENILLAS, A., RUBIERA, F., (1999), "Modelling NO<sub>x</sub> formation in coal particle combustion at high temperature: an investigation of the devolatilisation kinetics factors", *Fuel*, **78**, 1171.
- MAGNUSSEN, B., HJERTAGER, B., OLSEN, J. and BHADURI, D., (1979), *17th Symp. (Intn'l) Combust.*, 1383.
- RANZ, W. and MARSHALL, W., 1952, "Evaporation from Drops: Part I", *Chem. Eng. Prog.*, **48**, 141.
- ROGERS, H. (2006), "BlueScope Steel Phase II Blast Furnace PCI Combustion Test Program", Internal BlueScope Steel Report.
- SAXEN, H., BRAMMING, M., WIKSTROM, J.O. AND WIKLUND, P., (2001), *Ironmaking Conf. Proc.*, 721.
- SCHILLER, L. and NAUMANN, A., (1933), "Über die Grundlegenden Berechnungen bei der Schwerkraftaufbereitung", *VDI Zeits*, **77**, 318.
- SHEN, Y.S., SHEN, F.M, ZHU, M. AND ZOU, Z.S., (2002), *International blast furnace lower zone symposium*, Wollongong, Australia, 2-1~2-12.
- SHENG, C.D., MOGHADDERI, B., GUPTA, R. and WALL, T.F., (2004), "A computational fluid dynamics based study of the combustion characteristics of coal blends in pulverised coal-fired furnace", *Fuel*, **83**, 1543-1552.
- STAINLAY, R. and BENNETT, P., (2001), "PCI coal-status and forecast", *1<sup>st</sup> International Meeting on Ironmaking*, Belo Horizonte, Brasil, September 24-26.
- UBHAYAKAR, S., STICKLER, D., ROSENBERG, C. and GANNON, R., (1976), "Rapid Devolatilization of Pulverised Coal in Hot Combustion Gases", *16<sup>th</sup> Symp. (Int.) Combust. /The Combust. Inst.*, 427.
- WALL, T.F., ELLIOTT, L., SANDERS, D., CONROY, A., (2001), "A review of the state-of-the-art coal blending for power generation", *Project 3.16 of CRC for Black Coal Utilisation*, The University of Newcastle.
- YU, A. and STANDISH, N., (1990), "A Study of Particle Size Distributions", *Powder Technology*, **62**, 101-118.